

# DRILL WEAR PREDICTION SYSTEM USING OF MOTOR CURRENT AND FUZZY LOGIC METHOD

A. Salimi<sup>1,\*</sup>, M. Zadshakoyan<sup>2</sup>, A. Ozdemir<sup>3</sup> and E. Seidi<sup>4</sup>

\* aydin952@gmail.com

Received: December 2011

Accepted: April 2012

<sup>1</sup> Department of Mechanical Engineering, Faculty of Engineering, University of Payame Noor. Tehran, Iran.

<sup>2</sup> Department of Manufacturing Engineering, Faculty of Mechanical Engineering, University of Tabriz, Tabriz, Iran.

<sup>3</sup> Mechanical Education Department, Faculty of Technical Education, University of Gazi, Ankara, Turkey.

<sup>4</sup> Department of Agricultural Engineering, Faculty of Agriculture, University of Payame Noor. Tehran, Iran.

**Abstract:** In automation flexible manufacturing systems, tool wear detection during the cutting process is one of the most important considerations. This study presents an intelligent system for online tool condition monitoring in drilling process. In this paper, analytical and empirical models have been used to predict the thrust and cutting forces on the lip and chisel edges of a new drill. Also an empirical model is used to estimate tool wear rate and force values on the edges of the worn drill. By using of the block diagram of machine tool drives, the changes in the feed and spindle motor currents are simulated, as wear rate increases. To predict tool wear rate in drill, Fuzzy logic capabilities have been used to develop intelligent system. The simulated results presented in MATLAB software show the effectiveness of the proposed system for on-line drill wear monitoring.

**Keywords:** Tool wear condition monitoring, current signal, Fuzzy logic

## 1. INTRODUCTION

Tool wear detection is one of the most important problems found during manufacturing in automated C.N.C machine tools. The reason for acquiring the drill wear information is to enhance the predictive capability to allow the machine operator to schedule tool change or regrind just in time to avoid underuse or overuse of tools, avoid shutdown of machines due to damage, and to minimize scrap or rework. On the other hand, drill wear affects the ability of the hole cutting system to satisfy specified performance characteristics, such as hole roundness, centering, burr formation at drill exit, and surface finish. Although, many researches have been performed for tool condition monitoring, there is no practical method to predict wear rate in drilling process without some problems and limitations [1].

There are two methods for online tool wear estimation in cutting process. These methods have been classified into direct (optical, radioactive and electrical resistance .etc.) and indirect (AE, motor current, cutting force, vibration, etc.) sensing methods, according to the sensors used [2]. Recent attempts have

concentrated on the developing of the methods based on indirect monitoring [3- 5]. Among direct methods, the most widely used method is optical method. There is a basic problem with this method that machining process must be stopped during measurement of the wear [5, 6]. Therefore, to solve this problem, indirect methods were developed. In these methods, tool wear monitoring is performed by measuring variables such as tool vibration, cutting force, acoustic emission, motor current, etc.

Among indirect methods used for detecting tool condition, motor current sensing is a major one. The major advantage of using the measurement of motor current to detect a malfunction in the cutting process is that the measuring apparatus does not disturb the machining process. Moreover, it can be applied in the manufacturing environment at almost no extra cost [6]. Some researchers measured the spindle and feed motor current to estimate the static torque and thrust, in order to detect the tool condition [7].

Among indirect methods used for detecting the tool condition, motor current sensing is a major one. Mannan and nilson [7], measured the spindle and feed motor current to estimate the static torque and thrust, in order to monitor the tool condition.

The major advantage of using the measurement of motor current to detect a malfunction in the cutting process is that the measuring apparatus does not disturb the machining process. Moreover, it can be applied in the manufacturing environment at almost no extra cost [5].

In on-line tool wear monitoring, there are two methods to obtain the value of feed and spindle motor currents during drilling process, one of them is using models and, another is, measuring the motor currents by sensors. By the methods based on analytical models, first, the values of cutting and thrust forces for a new drill are predicted by models, then the value of thrust and cutting forces of the worn drill is predicted by using of analytical and empirical models. Finally, the values of motor currents required for the drilling process are obtained based on the thrust and cutting forces of the worn drill, by using of block diagram of machine tool drives. For investigating the results, the drill wear values obtained for the certain amount of motor currents are processed by decision support system like fuzzy logic or neural network.

In this paper, first, analytical models for thrust and cutting forces in drilling are simulated and also validated by experimental results. Then, tool wear model is simulated by using of forces, as input values of block diagram of the wear model. Thereafter, the block diagram of the machine tool drives are simulated and current transition behavior for spindle and feed motor, are shown, comparing with wear graph. In the last, an intelligent system with two inputs of feed motor current and spindle motor current is proposed to predict the wear values during the machining process, using fuzzy logic technique. The simulation results presented with MATLAB software show the effectiveness of fuzzy logic system for on-line tool wear monitoring in drilling operations.

## 2. DYNAMICAL MODELS OF FORCE IN DRILLING

In this section an analytical-empirical method is used to obtain force models. This method has been developed by Chandrasekharan et al [8]. In this method, various parameters of process (chip

thickness, cutting angles, feed rate and etc) are applied to create the model.

The most commonly used drill in drilling process, is the conventional conical point drill and in this paper the force models are developed for this drill only (Fig.1). Significant parameters that describe the geometry of a conical drill are the diameter( $2R$ ), point angle( $2k$ ), helix angle ( $\alpha_n$ ), web thickness( $2w$ ), chisel-edge angle(cea) and clearance angle( $\beta_0$ ). The cutting action at the drill point can be divided into two distinct regions: the cutting lips and the chisel edge. Models that account for the forces in drilling process will be formulated for each of these regions [8].

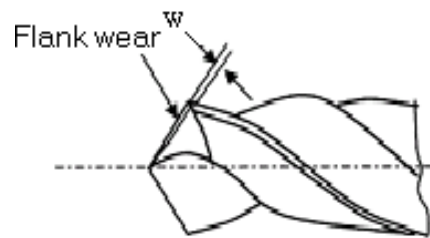


Fig.1. Schematic of a conical point drill [3]

### 2. 1. Cutting Lips Force Model Formulation

The cutting action along the cutting lips of a drill is a three-dimensional oblique cutting process. The cutting velocity, as well as the inclination, back rake, side rake and the normal rake angles, varies with the radial distance ( $r$ ) along the cutting lips of the drill. The radial distance is the distance of the point on the cutting lips from the drill axis measured in a plane that is normal to the axis. A normalized radial coordinate ( $\rho$ ) is defined such that  $\rho=r/R$ .

The equations that describe the above cutting parameters along the cutting lips as a function of the normalized radial distance have been developed by several researchers [8].

Experimental evidence has shown that the dependence of the specific cutting pressures on the chip thickness and cutting velocity is well described by Eq. (1) [8]. The specific cutting pressures can then be written as:

$$K_n = a_0 t_c^{a_1} v^{a_2} e^{a_3 a_n} \quad (1)$$

Since the equations describing the tangential cutting velocity and normal rake angle as a function of the normalized radial distance are known, the specific cutting pressure at points along the cutting lips can be computed if the coefficients for the chip thickness, velocity and normal rake angle are also known. These coefficients are typically determined experimentally. For machining operations with simpler tool geometries, such as turning and face milling, it is possible to design a simple set of experiments to determine these coefficients [8].

To facilitate a procedure for determining the coefficients of Eq. (1), an alternate formulation of the specific cutting pressures which exploits the geometric similarity of drills is used [8].

$$K_n(\rho) = C_1 \rho^a \quad (2)$$

Where  $C_1$  and  $a$  depend on the drill geometry and machining conditions. Writing the specific cutting pressures in the above form enables developing a closed form equation for the cutting forces. The elemental normal and tangential forces are now transformed to the elemental thrust and torque (Fig.2) and integrated between the appropriate limits to obtain the forces for any region on the cutting lips of drill. The thrust and torque force equations for the entire cutting lips are [8]:

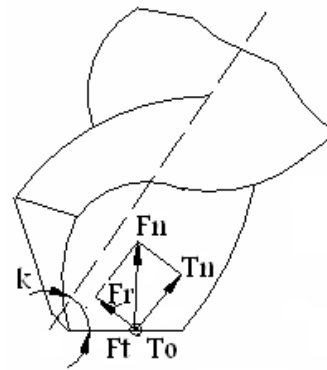


Fig. 2. Direction of forces acting on an element on the cutting lips [8]

$$T_l = F_n \sin k = \int_{\tau}^1 2k_n(\rho) \frac{f}{2} \sin k \cos i(\rho) R d\rho \quad (3)$$

$$T_o = \int_{\tau}^1 2k_r(\rho) \frac{f}{2} R \rho \cos i(\rho) R d\rho \quad (4)$$

Where  $\tau$  refers to the web length ( $2w/\sin(\pi - \text{cea})$ ) to diameter ratio. The inclination angle ( $i$ ) as a function of the normalized radial distance is given by:

$$i(\rho) = \sin^{-1} \left\{ \frac{w}{R\rho} \sin k \right\} \quad (5)$$

In Fig.3, the relationship between specific

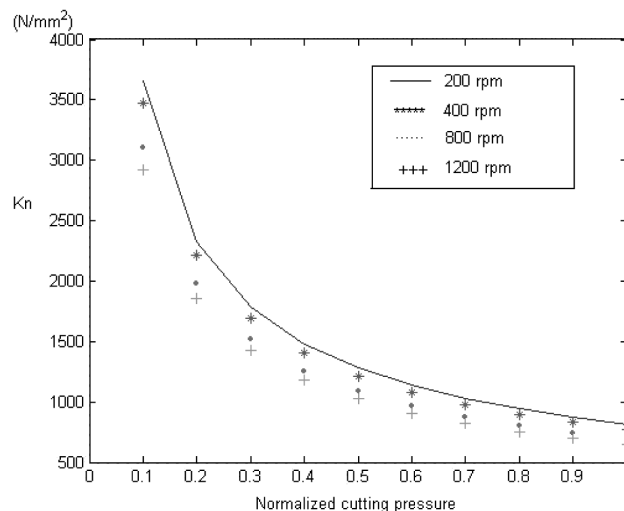


Fig. 3. Specific cutting pressure variation along the cutting lips in federate: 0.102 mm/rev

cutting pressure and normalized radial is shown. By obtaining the specific cutting pressure from the graph in Fig.3, the cutting and thrust force values can be estimated.

## 2. 2. Chisel edge Force Model Formulation

For drilling metals, in a small region around the center of the chisel edge, the tool does not actually cut but instead extrudes the material [8]. This region is called the extrusion or the indentation zone. In the region of the chisel edge outside the indentation zone (secondary cutting edges) orthogonal cutting with highly negative rake angle takes place (Fig.4).

Eq. (1) is used to determine the specific cutting pressures at the secondary cutting edges on the chisel edge. Since the chip thickness and the normal rake angle are constant along the chisel edge and only the tangential cutting velocity varies ( $V=2\pi Nr/60$ , where  $N$  is spindle speed in rpm), Eq. (1) can be modified and written in logarithmic form as [8]:

$$\ln K_n(r) = \ln a_0 + a_1 \ln t_c + a_2 \left\{ \ln \left( \frac{2\pi N}{60} \right) + \ln r \right\} + a_3 a_n \quad (6)$$

The normal rake angle at the chisel edge ( $\alpha_n$ ) is determined from the point angle and the chisel edge angle ( $cea$ ) of the drill by [8]:

$$\ln K_n(r) = \ln b_0 + b_1 \ln t_c + b_2 \left\{ \ln \left( \frac{2\pi N}{60} \right) + \ln r \right\} + b_3 a_n \quad (7)$$

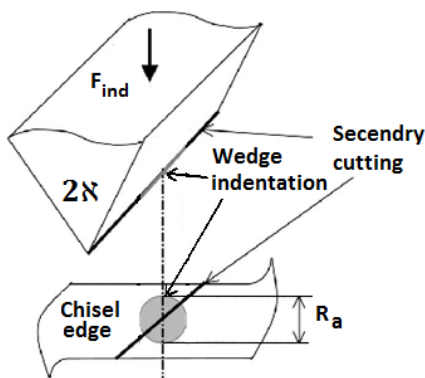


Fig. 4. Chisel edge of the drill [10]

$$\alpha_n = -\left\{ \tan^{-1} \left[ \tan(k) \cos(\pi - cea) \right] \right\} \quad (8)$$

The specific cutting pressures are integrated over the entire length of the chisel edge to obtain the thrust and the cutting force developed at the secondary cutting edges of the chisel edge.

To determine the cutting forces at the indentation zone for metals, the slip-line field method is used. The thrust and the torque forces due to the indentation zone is then given by [8]:

$$Th_i = \frac{4k(1 + \epsilon) f R_a \sin a_n}{[\cos a_n - \sin(a_n - \epsilon)]} \quad (9)$$

$$TO_i = \frac{2k(1 + \epsilon) f R_a^2 \sin a_n}{[\cos a_n - \sin(a_n - \epsilon)]} \quad (10)$$

Where  $\epsilon$  is determined from the boundary conditions of the problem and is computed from [3]:

$$2a_n(\text{rad}) = \epsilon + \cos^{-1} \left\{ \tan(\pi/4 - \epsilon/2) \right\} \quad (11)$$

$K$  is the yield shear stress of the workpiece material and is determined from experiments. By using of the equations, in this paper, Block diagrams (Fig.5) of the dynamical models of the forces in drilling process have been presented in MATLAB software. The simulation results have been given too. The results show the force changes along the chisel and lip edge (Fig.6 and 7).

## 3. TOOL WEAR MODEL

There is a straight relationship between force values and the wear rates. When the drilling process starts, the drill tool begins to wear and it causes the thrust and cutting forces to be increased, gradually. If the cutting tool cannot withstand the increased cutting forces, catastrophic tool failure becomes inevitable. Consequently tool life which is a direct function of tool wear is best determined by monitoring both cutting force and thrust force. Generally, thrust force and cutting force magnitudes are 50% larger when machining the last hole than when machining the first hole [9]. Moreover serious tool wear can cause 50% or 100%

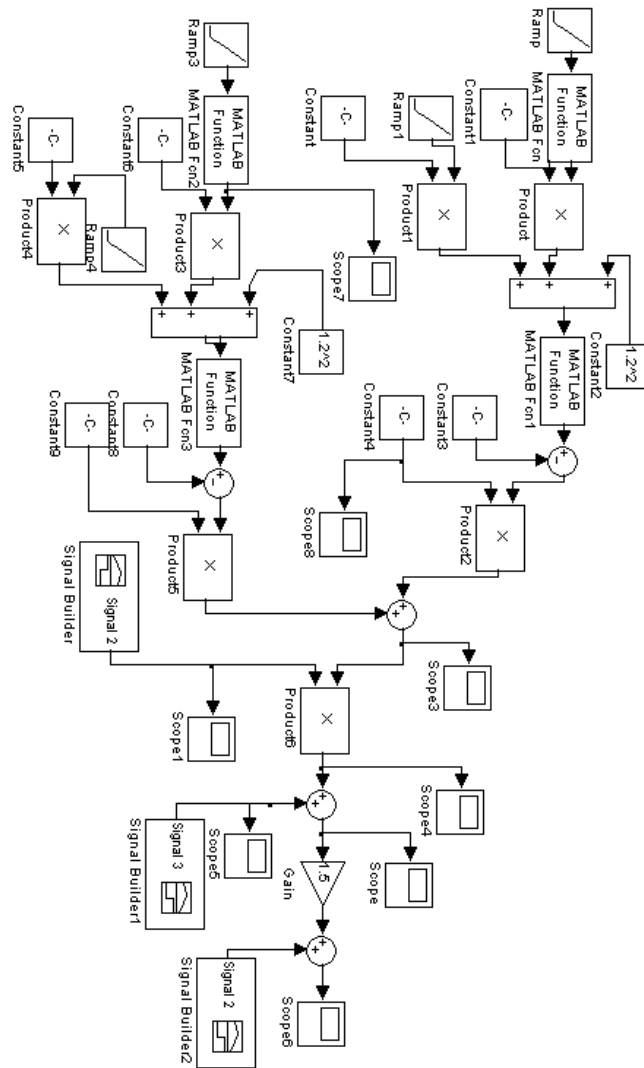


**Fig. 5.** Block diagram of dynamical thrust and cutting forces

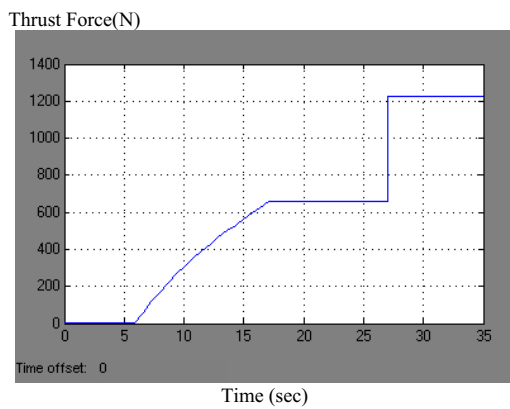


**Fig. 6.** Simulated thrust force diagram for a new drill: diameter 15.9 mm, point angle 118°, helix angle 33°, pilot hole diameter 3.2 mm, speed 200 rpm, federate 0.102 mm/rev

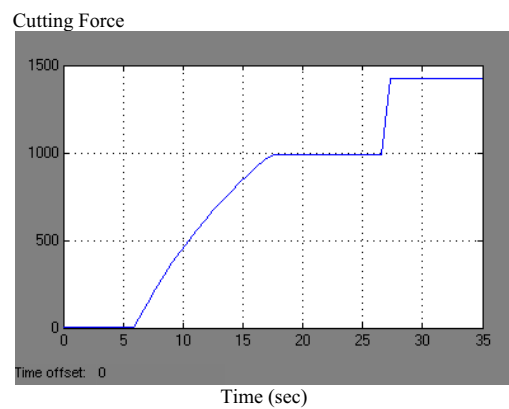


**Fig. 7.** Simulated cutting force diagram for a new drill: diameter 15.9 mm, point angle 118°, helix angle 33°, pilot hole diameter 3.2 mm, speed 200 rpm, federate 0.102 mm/rev

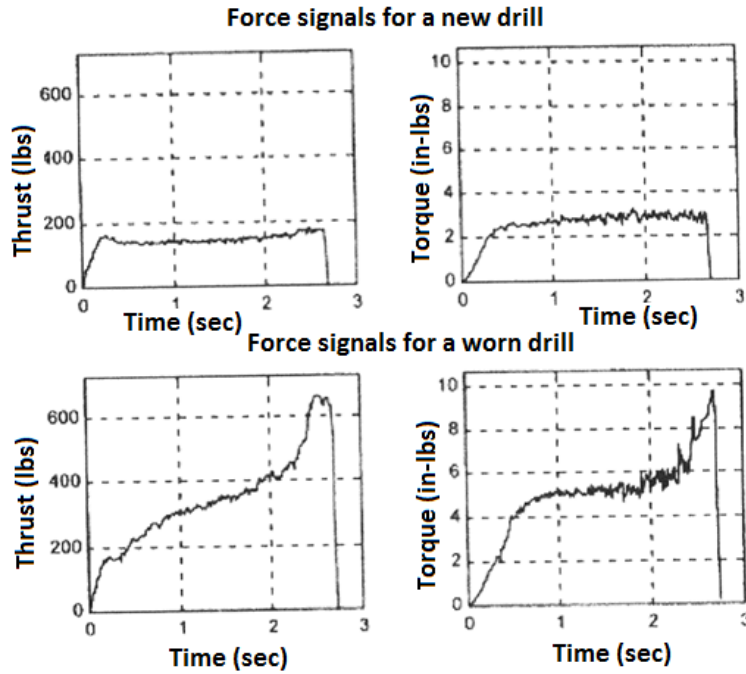


Fig. 8. Torque and cutting force changes in relation to the time [9]

increases in the amplitude of force signals [9]. Fig.8 illustrates the force signals for a new drill and a worn drill when drilling holes in a steel workpiece.

In general, the process of tool wear impairs the sharpness of the tools cutting edge, increases the friction between the tool and workpiece, and also increases the power consumption.

As it was mentioned above, when the machining operation is continued during the machining time, tool starts to wear and the force necessary for the operation continuation increases. The cutting force acting on the lip edge consists of two components: one of its components is created via machining operation ( $F_{cut}$ ) and the other is created from friction between the tool and the work piece. Therefore the total force is [3]:

$$F = F_{cut} + kw b \quad (12)$$

In the formula.(12), k, is a constant value, w, is the wear rate and b, is cutting length. Dynamical models of the forces for a new tool have been investigated in references [10, 8].

To analyses the relationship between the wear

and force rates, the wear model should be developed. The wear model parameters must be estimated by experimental results. State equations for the tool wear model have been developed in [11]. In this equations,  $K1$ ,  $K0$ ,  $K2$ ,  $C_w$ ,  $\alpha$ ,  $\tau$  are the model parameters that are related to the machining conditions. The methods of estimating these parameters have been given in [11]. In this model:  $X1$  is diffusion wear  $X2$ : initial wear  $X3$ : linear wear  $Wf1$ : composed of two initial and linear wear  $Wf2$ : is diffusion wear that increases with rising the temperature.  $F_0$  is the cutting force and  $F_c$  is the total force with respect to the wear effect and, s, in this model is the Laplace variable. Block diagram of the wear model has been shown in Fig.9. Also Fig.10 and Fig.11 show the effects of the drill wear on the cutting and thrust forces. The results have been simulated in MATLAB software. The state equations of wear model are:

$$\dot{X}1 = aK2Cw(X1 + X2 + X3) + K2F_0 \quad (13)$$

$$\dot{X}2 = \frac{1}{\tau}(K_0F_0 - X2) \quad (14)$$

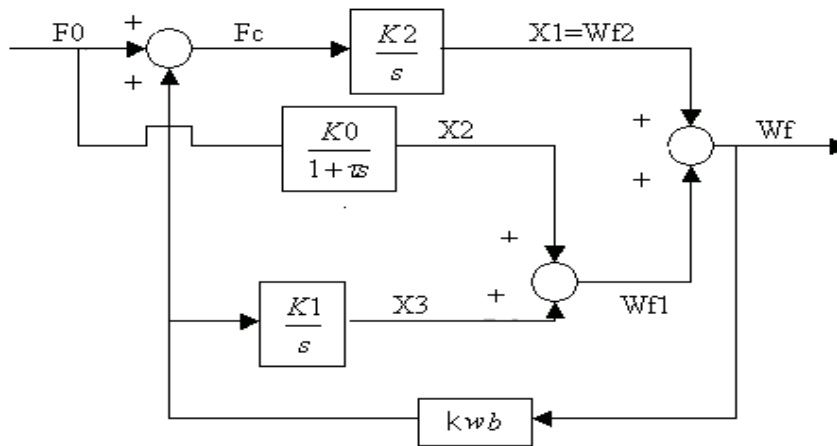


Fig. 9. Block diagram of the wear model [11]

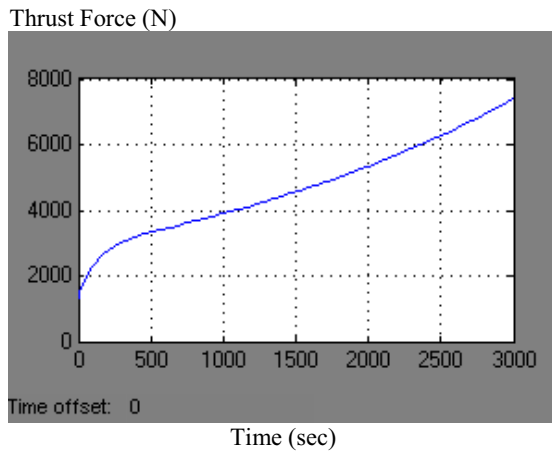


Fig. 10. Simulated thrust force diagram for a worn drill: diameter 15.9 mm, point angle 118°, helix angle 33°, pilot hole diameter 3.2 mm, speed 200 rpm, federate 0.102 mm/rev

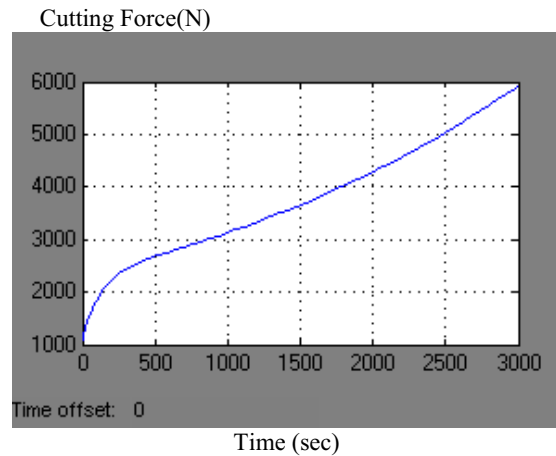


Fig. 11. Simulated cutting force diagram for a worn drill: diameter 15.9 mm, point angle 118°, helix angle 33°, pilot hole diameter 3.2 mm, speed 200 rpm, federate 0.102 mm/rev

$$\dot{X}_3 = aK_1C_w(X_1 + X_2 + X_3) \quad (15)$$

$$F_c = F_0 + bC_wW_f \quad (16)$$

#### 4. EXPERIMENTAL SET-UP

Drilling experiments were conducted on an OKUMA (MC-4VAE) CNC machining center. A kistler (9273 A), Four-channel dynamometer was used to measure the thrust and torque forces. Material used is gray cast iron. Data has been

sampled at 100Hz and stored in a pc. Table 2 shows the parameters used in this paper [8].

#### 5. DRIVE SYSTEMS

Feed drive system of the motor makes the proportional movement between the work piece and the cutting tool. In Fig.12, the feed drive system of the machine tool has been shown. The axis of feed drive system is the positioning device for the relative movement between the work piece and the cutting tool. It transforms the voltage  $V_m$  via the servo system into the corresponding feed rate.

**Table2.** Experimental results of the torque and the thrust force [8]

| Feed (mm/rev) | Speed (rpm) | Diameter (mm) | Point angle | Web Thickness (mm) | Pilothole Diameter (mm) | Cutting lips |             | Total chisel |        | Entire drill |             |
|---------------|-------------|---------------|-------------|--------------------|-------------------------|--------------|-------------|--------------|--------|--------------|-------------|
|               |             |               |             |                    |                         | Thrust (N)   | Torque (nm) | Thrust (N)   | torque | Thrust (N)   | Torque (Nm) |
| 0.229         | 400         | 15.9          | 118         | 2.3                | 3.2                     | 1091.5       | 13.52       | 1037         | 1.29   | 2228         | 14.8        |
| 0.102         | 200         | 15.9          | 118         | 2.3                | 3.2                     | 661.5        | 7.31        | 629          | .548   | 1352         | 8.63        |
| 0.102         | 800         | 15.9          | 118         | 2.3                | 3.2                     | 574.8        | 6.85        | 503          | .505   | 1149         | 7.36        |
| 0.254         | 400         | 12.7          | 118         | 2.3                | 2.8                     | 953.0        | 9.34        | 863          | .919   | 1873         | 10.2        |
| 0.102         | 400         | 9.5           | 118         | 1.5                | 2.4                     | 373.5        | 2.7         | 393          | .356   | 811          | 3.06        |
| 0.102         | 400         | 12.7          | 118         | 2.3                | 2.8                     | 490          | 4.9         | 510          | .7     | 1000         | 5.7         |
| 0.102         | 400         | 15.9          | 135         | 2.3                | 4.4                     | 539.8        | 4.42        | 299          | .468   | 868          | 6.86        |
| 0.178         | 400         | 9.5           | 118         | 1.5                | 2.4                     | 525.4        | 8.11        | 743          | .601   | 1376         | 8.72        |

In this part, the linear model of the drive is described by developing the linear equations between the motor and components of the drive mechanism and then, by taking the Laplace transforms with zero initial condition. Nonlinearities such as coulomb friction and backlash are included in the model too.

To create the total model of feed system, it is necessary to analysis the dynamical equations of the feed drive and D.C servomotor. By taking attention to the Fig.12 and Fig.13, the equations of motion are [12]:

$$T_G - (p_1 - p_2) r_1 - B_1 s \theta_1 = j_1 s^2 \theta_1 \quad (17)$$

$$T_D - (p_1 - p_2) r_2 - B_2 s \theta_2 = j_2 s^2 \theta_2 \quad (18)$$

$B_1, B_2$  in the above, respectively, are viscose friction constant of the motor pulley, motor bearing and ball screw bearing, and its pulley.  $j_1, j_2$  respectively, are motor and its pulley moment, also, ball screw and its pulley moment inertia.  $\theta_1, \theta_2$  respectively, are the motor pulley and ball screw pulley locations.  $p_1, p_2$  are the belt forces.  $T_G$  is the initial torque produced by the motor armature. The drive torque,  $T_D$  overcomes the axial force in the ball-nut due to the table inertia and friction, and the resulting force  $F_D$  causes the table to slide along the sideways at required

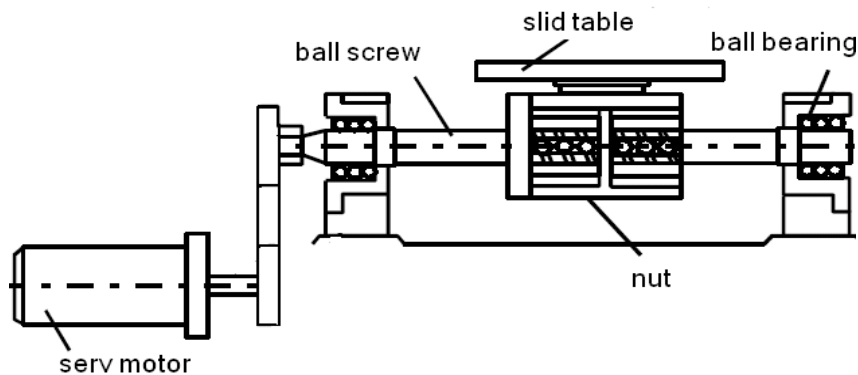


**Fig. 12.** Machine tool feed drive system [15]



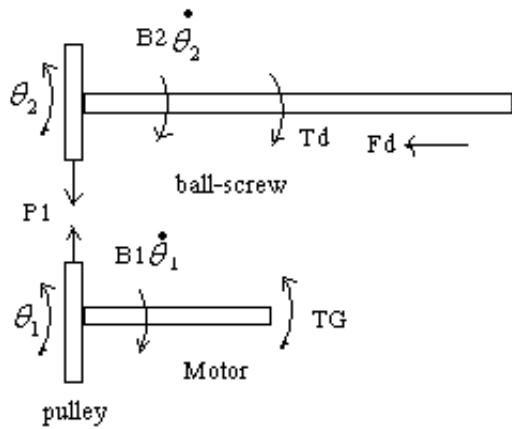


Fig.13. Model of motion [12]

velocity. The required torque on the ball screw to overcome the axial drive force is:

$$T_D = \left( \frac{h_{sp}}{2\pi\mu} \right) F_D \quad (19)$$

Where  $h_{sp}$ , is the pitch or lead of the ball-screw and  $\mu$  is the ball screw efficiency. The input voltage to the motor is  $V_m$  that after overcoming the voltage of feedback loop causes a time lagged motor current  $I$ . In a permanent magnet DC motor, the current produces a proportional torque  $T_G$ .

In Fig.14, spindle drive system of the drilling machine has been shown in which the motor shaft is joined to spindle shaft by means of the belt and transforms the revolving motion.  $T_b$ , in Eq. (20) is viscous damper torque.  $\theta, j, B$  respectively is the spindle radial speed, inertia moment and viscous friction constant of the pulley and spindle. In this

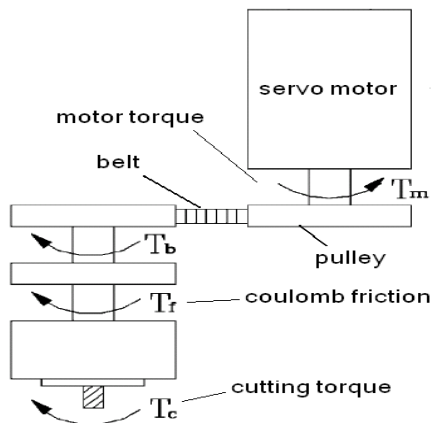


Fig.14. Spindle drive system of the drilling machine [3]

paper all of the parameters for spindle and feed drive systems have been obtained for IHU3 type of the motor. Equation for spindle system is [3]:

$$T_m = js^2\theta + Bs\theta + T_f + T_b \quad (20)$$

Block diagrams of the feed and spindle drive systems for the drilling machine tool have been shown in Fig.15 and 16. The drive systems are simulated in MATLAB software and the feed and spindle motor current changes, are extracted

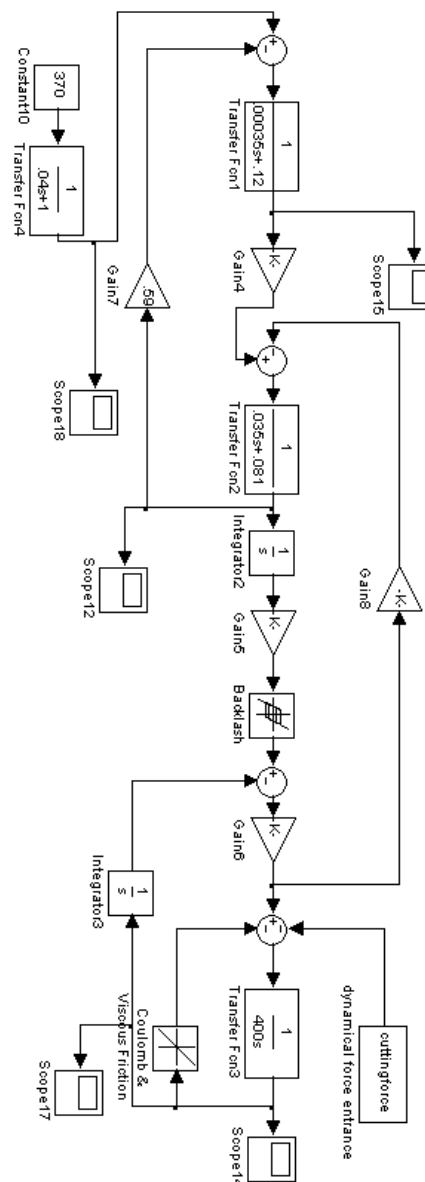


Fig. 15. Simulated block diagram of feed drive for the IHU3 type of motor

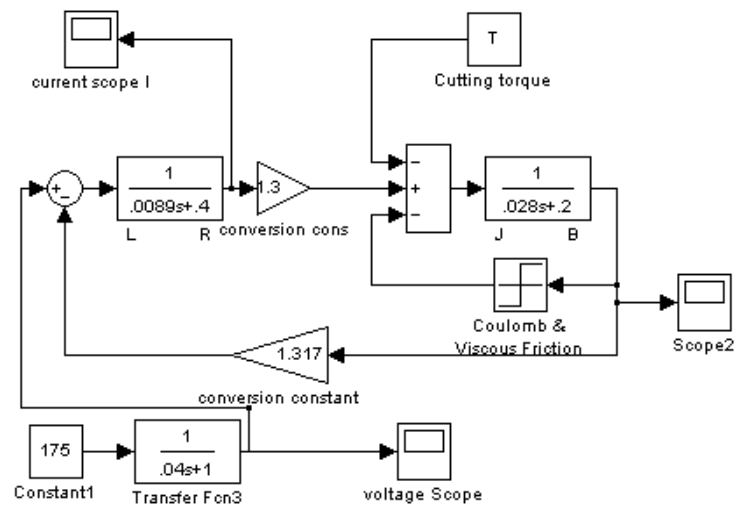


Fig. 16. Simulated block diagram of spindle drive for IHU3 type of motor

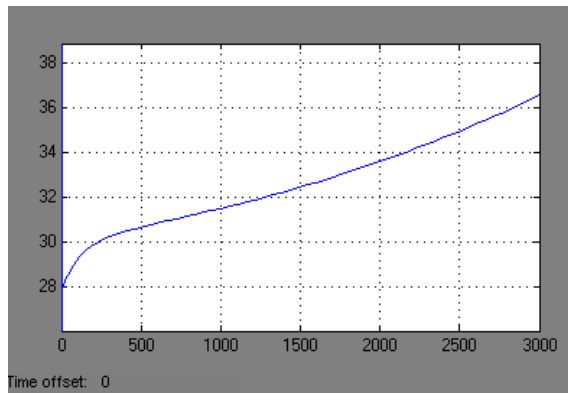


Fig. 17. Simulated feed motor current diagram during drilling: diameter 15.9 mm, point angle 118°, helix angle 33°, pilot hole diameter 3.2 mm, speed 200 rpm, federate 0.102 mm/rev

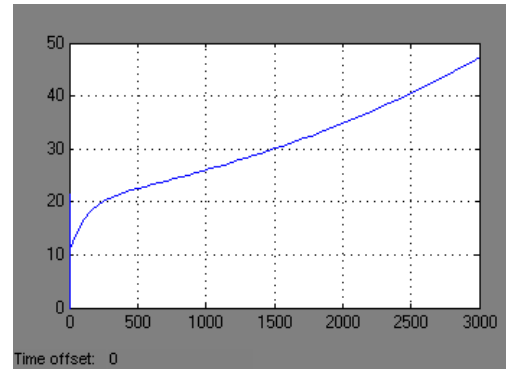


Fig. 18. Simulated spindle motor current diagram during drilling: diameter 15.9 mm, point angle 118°, helix angle 33°, pilot hole diameter 3.2 mm, speed 200 rpm, federate 0.102 mm/rev

during the drilling process (Fig.17 and Fig.18). As is seen in the simulated results, drill wear results in increase in the feed and spindle motor currents during the machining operation. Also, the relationship between the force and motor current follow the same behavior.

## 6. FUZZY LOGIC

Zadeh [13] introduced fuzzy logic for the first time in 1965. Fuzzy logic is a major development of fuzzy set theory. This is a multi-valued logic that allows intermediate values to be defined between conventional evaluations like yes/no,

black/white, etc. In contrast with traditional logic theory, where binary sets have two-valued logic: true or false, fuzzy logic variables may have a truth value that ranges in degree between 0 and 1. Fuzzy logic has been extended to handle the concept of partial truth, where the truth value may range between completely true and completely false. Furthermore, when linguistic variables are used, these degrees may be managed by specific functions. In other words, fuzzy logic was designed to represent and reason with knowledge in linguistic or verbal form. As an extension of the case of multi-valued logic, valuations ( $\mu, v_0 \rightarrow w$ ) of propositional variables

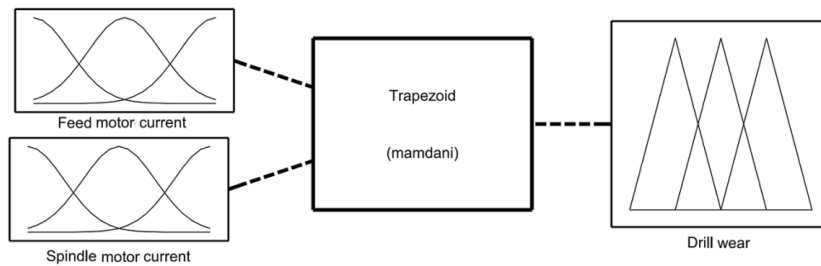


Fig. 19. Fuzzy logic model designed for drill wear prediction

( $v_0$ ) into a set of membership degrees ( $w$ ) can be thought of as membership functions mapping predicates into fuzzy sets (or more formally, into an ordered set of fuzzy pairs, called a fuzzy relation). With these valuations, many-valued logic can be extended to allow for fuzzy premises from which graded conclusions may be drawn.

Decisions in fuzzy systems are based on inputs in the form of linguistic variables. The variables trigger, or „fire”, a certain number of IF-THEN rules, which produce one or more responses (conclusions) depending on which rules are fired. The conclusion of each rule is weighted according to the degree of membership of its inputs. Usually, the centre of gravity of the responses is calculated to obtain an appropriate crisp output. The major advantages of the fuzzy logic approach are: i) a mathematical model is not necessary, ii) the knowledge base is formed by a set of practical rules using linguistic variables, and iii) this method is very efficient under uncertain conditions, which are common in everyday situations. According to Li and Elbestawi [14], fuzzy logic is the preferred algorithm because it is capable of providing a systematic means for dealing with the inherent uncertainties in the nonlinear processes.

### 6. 1. Fuzzy Logic Modeling

To predict the wear rate in this research, fuzzy logic toolbox in MATLAB software was used. The fuzzy inference system predicts the amount of drill wear due to the changes in motor currents. Two parameters including the spindle and feed motor currents were given to the fuzzy model as inputs and the values of drill wear rate were determined as the output. In order to obtain an

accurate result, all of the existed membership functions in MATLAB, were tried and the best function was used for fuzzy modelling. In this research the mamdani method was applied to design the fuzzy logic model and the Trapezoid and Triangular membership functions are selected. After entering the inputs and outputs in the model, the rule base system must be designed to control the system. As mentioned previously in this paper, the knowledge base or rule base system is designed based on the experimental data. The larger the number of experiments the more accurate results will be obtained. In this research, the number of rules is 36 by which the input and output are connected to each other. Fig. 19 shows the fuzzy logic model in which the spindle and feed motor current values are as inputs, and wear rates are as output. The membership functions of the wear model are seen in Fig.20, 21, 22.  $w_1$  in Fig.22 is the minimum wear rate in which, the tool is assumed to be sharp and  $w_8$  is the maximum wear rate in which, the tool is supposed to be worn out and breakage probability is very high. The wear region is divided to 8 small regions. The wear rate for the new drill is taken between 0 and 0.15mms and the wear rate for a worn drill are taken between

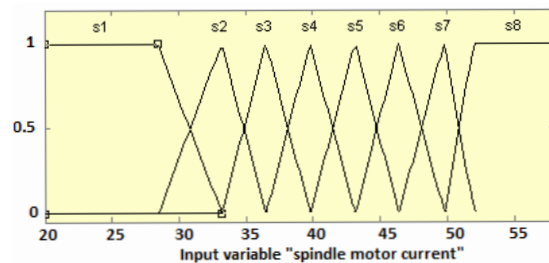


Fig. 20. Spindle current membership function

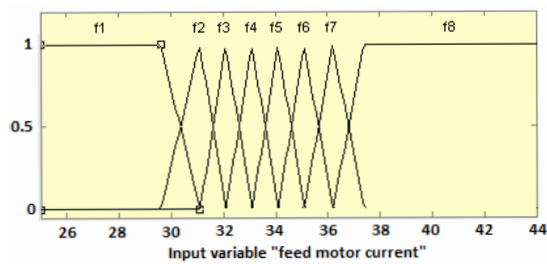


Fig. 21. Feed current membership function

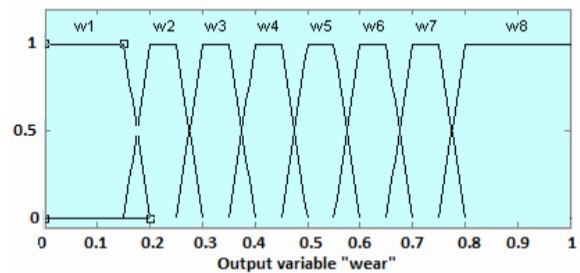


Fig. 22. Drill wears membership function

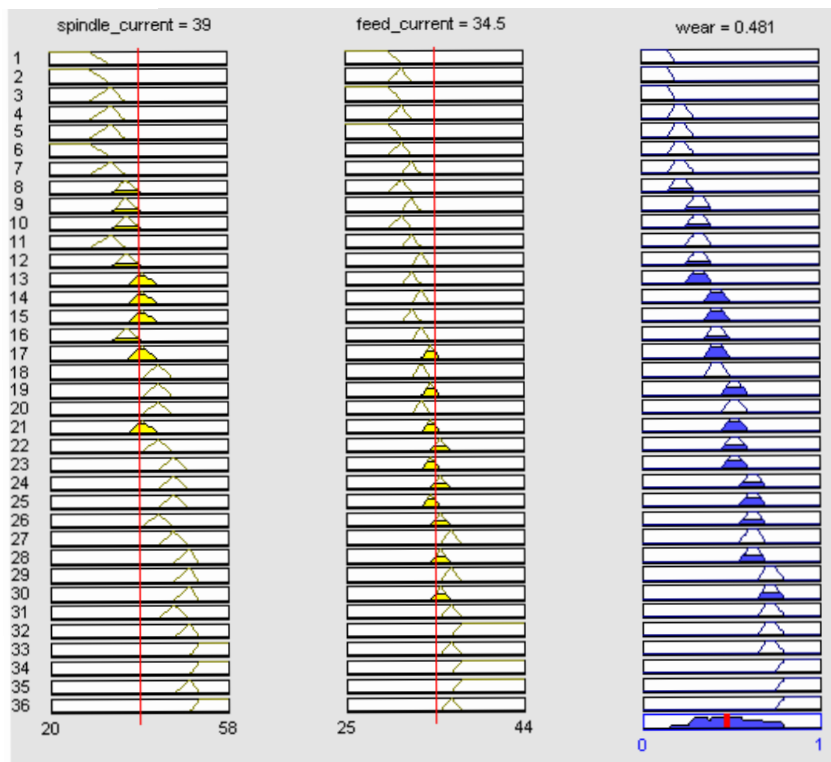


Fig. 23. Fuzzy rule base system

0.8mm and 1mm. When the wear rate reaches to 0.8mm it means that the tool must be changed with a new one. The wear rate of 0.8mm is only used for HSS drills and for the carbide tools the tool life is taken less than 0.35mm. Drill wear prediction system is presented in Fig.23. In this model when the values of the feed and spindle currents are changed during the drilling process drill wear rate can be predicted by on-line. The wear rate obtained from the analytical model is then compared to the estimated wear rates obtained from fuzzy model. When the wear rate

reaches to the expected values at which the drill should be changed, a signal is sent to the machine tool control system to stop the process. The block diagram of the fuzzy control system is given in Fig.24. To extract the reliability of the system the results predicted by the fuzzy logic model are compared with the results obtained from the analytical models. As seen in Fig.25, the results show that there is a closeness compromise between the results as the value of R2 of regression graph is 0.9367.

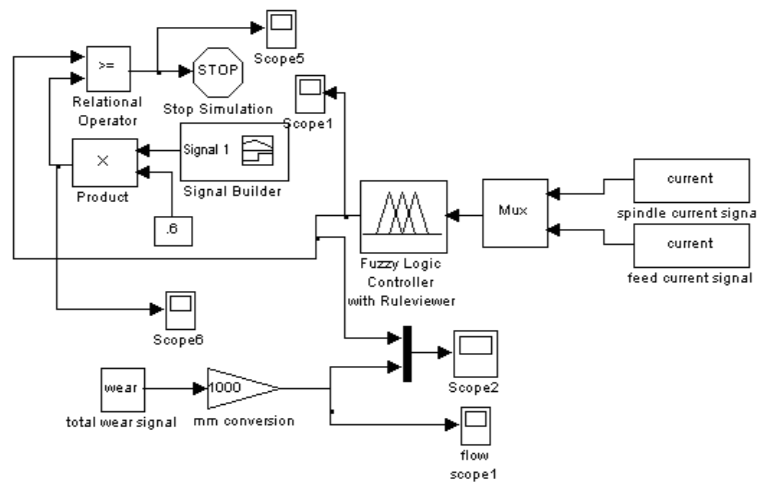


Fig. 24. Simulated model of the fuzzy logic system

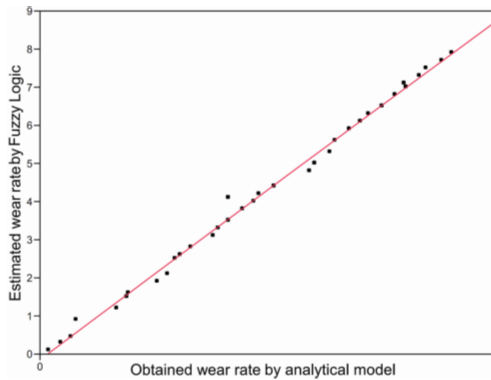


Fig. 25. Comparison of the wear rate obtained from fuzzy logic and analytical model

## 7. RESULTS AND CONCLUSION

In this paper an intelligent system for drill wear prediction is proposed. For this purpose, first the analytical and empirical models of cutting and thrust forces are used to simulate the dynamical forces in lip and chisel edges of the drill. Then a wear model is used to predict tool wear rate in any arrangements and also machine tool drive block diagram is used to predict feed and spindle motor current rate. Finally the data were investigated by a fuzzy logic system and the results compared to each other.

Instead of the machine tool in this paper, block diagram of the machine tool used to predict the amount of motor currents. For this purpose three

models including the thrust and cutting force block diagram, tool wear model block diagram and the machine tool drive system block diagram are connected to each other to give the motor current changes in relation to the cutting and thrust forces of the drill during drilling process.

Predicting and monitoring of the drill wear rate by using of feed and spindle current motor is possible and can be applied widely in adaptive control systems to prevent drill wear failure. Also, the fuzzy logic system is an important and effective tool to investigate and predict the nonlinear incidents, like tool wear, in machining systems.

Using of analytical models and control system of the machine tool is one of the specifications of this paper that can be used even as a sensor less method to detect and monitor the machining process. In the case of facing with any problem during the machining process the current behavior can be analyzed and followed through system block diagram.

## 8. ACKNOWLEDGMENT

The work was supported by the Peyame noor University of Tabriz. The supports are gratefully acknowledged.

## REFERENCES

1. Zhang, M. Z., Liu, Y. B. and Zhou, H., "Wear

**Table 1.** Nomenclature used in the research

|             |   |               |                                |
|-------------|---|---------------|--------------------------------|
| $F_n$       | Normal force                                      | $cea$         | Chisel- edge angle             |
| $f(mm/rev)$ | Feed rate   | $f_s(mm/sec)$ | Feed rate                      |
| $i$         | Inclination angle                                 | $K$           | Yield shear stress             |
| $k_n$       | Normal specific cutting pressure                  | $2k$          | Point angle                    |
| $2R$        | Drill diameter                                    | $R_a$         | Radius of the indentation zone |
| $r$         | Radial distance of an element on the cutting lips | $r_p$         | Pilot hole radius              |
| $Th_{ct}$   | Cutting lips thrust force                         | $Th_i$        | Indentation zone thrust force  |
| $t_c$       | Uncut chip thickness                              | $v$           | Tangential cutting velocity    |
| $2w$        | Web thickness                                     | $\alpha_0$    | Helix angle                    |
| $\alpha_n$  | Normal rake angle                                 | $\alpha_1$    | Chisel edge normal rake angle  |
| $\beta_0$   | Clearance angle                                   | $\tau$        | Web length- to diameter ratio  |
| $k_t$       | Tangential specific cutting pressure              | $T_o$         | Cutting lips torque            |
| $To_i$      | Indentation zone torque                           | $b$           | Cutting length                 |

mechanism maps of uncoated HSS tools drilling die-cast,” Aluminum Alloy Tribology International, 34 , 727–731,2001.

- Jantunen, E., “A summary of methods applied to tool condition monitoring in drilling,” International Journal of Machine Tools & Manufacture, 42, 997–1010, 2002.
- Kim, H. Y., Ahn, J. H., Kim, S. H. and Takata, S., “Real-time drill wear estimation based on spindle motor power,” Journal of material processing technology , 124, 267-273, 2002.
- Xiaoli, Li. and Tso, S. K., “Drill wear monitoring based on current signals,” Elsevier Wear, 231, 172-178, 1999.
- Xiaoli, Li., Shiu, Kit. Tso. and Jun, Wang., “Real – time tool condition monitoring using wavelet transform and fuzzy techniques,” Systems, Man, and Cybernetics, Part C: Applications and Reviews, IEEE Transactions on, 30, 352-357, 2000.
- Xiaoli, Li., Xinping, G. and Hongrui, W., “Identification of tool wear states with fuzzy classification,” International Journal of Computer Integrated Manufacturing, 12, 503-509, 1999.
- Mannan, M. A., Nilsson, T., “The behavior of static torque and thrust due to tool wear in boring, Technical papers of the North American Manufacturing Research Institution of SME,” 1, 75-80, 1997.
- Chandrasekharan, V., Kapoor, S. G. and Devor, R. E., “A mechanistic approach to predicting the cutting forces in drilling: with application to fiber-reinforced composite materials”, Journal of Engineering for Industry, 117, 559-570, 1995.
- Ertunc, H. M. and Loparo, K. A., “A decision fusion algorithm for tool wear condition monitoring in drilling,” International Journal of Machine Tools and Manufacture, 41, 1347-1362, 2001.
- Juhchin, A., Venkatraman, Yang. and Jaganathan, Ruxu. Du., “A new dynamic model for drilling and reaming processes,” International Journal of Machine Tools & Manufacturing , 42, 299-311, 2002.
- Carrillo, F. J. and Zadshakoyan, M., “Adaptive observer for on-line tool wear estimation and monitoring in turning,” using a hybrid identification approach ECC’97 European

- Control Conference. Bruxelles, Belgique, 1, 1-4, 1997.
12. Ebrahimi, M. and whalley, R., "Analyses, modeling and simulation of stiffness in machine tool drives," *Computer & Industrial Engineering*, 38, 93-105,2002.
  13. Zadeh L. A., "Fuzzy set", *Information Control*, 8, 338– 353, 1965.
  14. Li S., Elbestawi M. A., "Tool condition monitoring in machining by fuzzy neural networks," *Journal of Dynamic Systems, Measurement, and Control*, 118, (1996), 665–672.
  15. Atsushi, M., Yoshiaki, K. and Yasumi, W., "Servo performance enhancement of high speed feed drives by damping control," *Proc. of Japan US Sympo. on Factory Automation (JUSFA2000)*, Ann Arbor, Michigan,1,2000.